Pressure-Induced Phase Transition in $PbSc_{0.5}Ta_{0.5}O_3$ as a Model Pb-Based Perovksite-Type Relaxor Ferroelectric

B. Mihailova,[1,*] R. J. Angel,[2,†] A.-M. Welsch,[1] J. Zhao,[2] J. Engel,[2] C. Paulmann,[1] M. Gospodinov,[3] H. Ahsbahs,[4] R. Stosch,[5] B. Güttler,[5] and U. Bismayer[1]

[1]*Mineralogisch-Petrographisches Institut, Universität Hamburg, Grindelallee 48, 20146 Hamburg, Germany*
[2]*Virginia Tech Crystallography Laboratory, Department of Geosciences, Virginia Tech, Blacksburg, Virginia 24060, USA*
[3]*Institute of Solid State Physics, Bulgarian Academy of Sciences, Boulevard Tzarigradsko Chausse 72, 1784 Sofia, Bulgaria*
[4]*Institut für Mineralogie, Petrologie und Kristallographie, Universität Marburg, Hans-Meerwein-Straße, 35032 Marburg, Germany*
[5]*Physikalisch-Technische Bundesanstalt, Bundesallee 100, 38116 Braunschweig, Germany*

We report pressure-induced structural changes in $PbSc_{0.5}Ta_{0.5}O_3$ studied by single-crystal x-ray diffraction and Raman scattering. The appearance of a soft mode, a change in the volume compressibility, broadening of the diffraction peaks, and suppression of the x-ray diffuse scattering show that a phase transition occurs near $p_c \sim 1.9$ GPa. The critical pressure is associated with a decoupling of the displacements of the B site and Pb cations in the existing polar nanoregions, leading to the suppression of B-cation off-center shifts and enhancement of the ferroic distortion in the Pb-O system.

Relaxors are ferroelectrics with a broad, frequency-dependent maximum of the dielectric permittivity over a temperature range and a number of technological applications [1]. The majority of relaxors are Pb-based perovskite-type oxides of the general formula $(Pb, A)(B', B'')O_3$. Relaxor behavior is related to the rather complex nanoscale structure of these materials. Polar nanoclusters occur at temperatures well above the temperature of dielectric-permittivity maximum T_m, whereas at low temperatures the ferroic distortion of the unit cell is very weak and often unresolved by diffraction methods. Near T_m the structural state of relaxors consists of dynamic polar nanoclusters (life time $\sim 10^{-5}$–10^{-6} s) incorporated into a paraelectric matrix. The mechanism of nucleation and growth of polar nanoclusters, as well as the reason for the suppression of long-range ferroelectric ordering below T_m, is not yet clear.

High-pressure (HP) structural studies can help to resolve the complexities in relaxors, because mechanical loading can slow down the dynamic structural fluctuations. Two general features have emerged from the limited number of HP experiments of relaxors. First, there is a pressure-induced crossover from normal-ferroelectric to relaxor-ferroelectric state revealed by dielectric-permittivity experiments at moderate pressures (up to 1.5 GPa), which has been assumed to result from a decrease in the correlation length between polar clusters under pressure [2]. Second, the x-ray diffuse scattering which is typical of relaxors at ambient pressure, and results from the polar nanoclusters [3] is suppressed at HP [4]. The origin of this second phenomenon is still not well understood. The simplest explanation that it reflects the suppression of ferroic displacements is inconsistent with the observed Raman scattering [4,5]. The observations are, however, consistent with either the formation of long-range ferroic ordering or complete disordering of the ferroic displacements.

We chose to study $PbSc_{0.5}Ta_{0.5}O_3$ (PST) as a model Pb-based perovskite-type relaxor because (i) the stoichiometry is consistent with 1:1 B-cation compositional order along $\langle 100 \rangle$, which, on the local scale, is a common relaxor feature [6], (ii) below T_m PST shows long-range ferroelectric ordering, which suggests larger polar nanoclusters in the vicinity of T_m as compared to canonical relaxors, and (iii) at ambient pressure T_m is close to room temperature. Thus at ambient temperature relaxor features are well developed in PST, which should facilitate the detection of pressure-induced structural changes. In this Letter we demonstrate that the strong decrease in the diffuse scattering at a critical pressure is associated with a structural elastic instability involving a continuous change in the pseudocubic volume compressibility and the appearance of a soft mode. The HP phase is characterized by loss of coherence between the sublattices of B cations and Pb atoms; the former becomes "less distorted," while the latter "more ferroic."

Single crystals of partially B-site ordered PST (mean size of B-site ordered regions ~ 6 nm, $T_m \sim 280$ K at ambient pressure) were synthesized by the high-temperature solution growth method. Raman scattering experiments were conducted with a Horiba Jobin-Yvon T64000 equipped with a microscope. The as-measured spectra were subsequently reduced by the Bose-Einstein phonon occupation factor. The unit-cell parameters were measured with a laboratory 4-circle diffractometer [7]. Single-crystal x-ray diffraction (XRD) experiments with synchrotron radiation were performed at the $F1$ beam line at HASYLAB/DESY, using a wavelength of 0.4000 Å and a MarCCD 165 detector. All of the HP measurements were conducted at ambient temperature in diamond anvil cells. Pressure media of 16:3:1 methanol-ethanol-water and 4:1 methanol-ethanol were used in the spectroscopic and diffraction experiments, respectively, assuring hydrostatic-

pressure conditions in the experimental pressure range to 9.0 GPa [8]. The ruby-line luminescence method was used to determine the pressure in the spectroscopic and synchrotron-based XRD experiments [9], while quartz was used as internal pressure standard for the in-house XRD experiments [7].

In-house single-crystal XRD measurements showed that at ambient and low pressures the diffraction maxima with h, k, l all even [indexed on the double-perovskite (8 Å) cell, $Fm\bar{3}m$] are sharp, and the measured unit-cell parameters are cubic. At pressures above 1.9 GPa the diffraction maxima show broadening (Fig. 1), which was completely reversible on pressure release. The broadening cannot represent a decrease in domain/crystallite size because the corresponding reflections arise from the average cubic structure alone. At the same pressure the evolution of the unit-cell volume V of the material shows a distinct change (Fig. 2). This change in elasticity is clearer when the data are transformed to an "f-F" plot (Fig. 2) in which the normalized pressure $F_E = p/3f_E(1 + 2f_E)^{5/2}$ is plotted against the Eulerian finite strain, $f_E = [(V_0/V)^{2/3} - 1]/2$. The low-pressure data indicate that the bulk modulus K_T of the material is *decreasing* with *increasing* pressure. At $p > 2$ GPa the slope of the f-F plot is positive, and a direct fit of the p-V data indicates that $dK_T/dp = 13 \pm 4$. There is no detectable discontinuity in the unit-cell volume (Fig. 2), but there is in the bulk modulus (Fig. 2). These observations are all characteristic of a thermodynamically second-order structural phase transition involving elastic softening in both phases as they approach the phase transition [10].

The low-pressure diffraction patterns (Fig. 3) reconstructed from the synchrotron x-ray scattering data contain the same classes of Bragg reflections with $h, k, l =$ all even and $h, k, l =$ all odd found at ambient conditions, corresponding to an apparent $Fm\bar{3}m$ symmetry of the average structure. The ⟨110⟩ diffuse streaks This peak is generated by rhoresulting from atomic displacements in polar nano-regions [3] decrease in intensity when approaching p_c, but at $p > p_c$ the streaks still persist in weakened form, suggesting that correlated atomic displacements remain in the

sample at least up to 2.8 GPa. With increasing pressure up to $p_c = 1.9$ GPa the intensities of certain reflections with $h + k + l = 4n + 2$ (n integer) decrease continuously (Fig. 3). Structure factor calculations suggest that this can only result from antiferroic displacements of the Pb atoms in the *average* structure. The absence of new classes of reflections at high pressures eliminates the possibility of a transition to a structure in which the BO_6 octahedra are tilted in-phase [11]. However, the structure could develop an antiphase tilt system as that would only contribute small changes to the intensities of the $h, k, l =$ all odd reflections [11]. Thus, the symmetry change of the double-perovskite framework alone is restricted to be from $Fm\bar{3}m$ to either $R\bar{3}$, $I4/m$, or $C2/m$ [11]. Space group $C2/m$ is, however, excluded by the thermodynamically continuous character of the transition. If the tilt pattern corresponds to $R\bar{3}$ symmetry, then the presence of antiferroic Pb displacements deduced from the change in the intensities of the $h + k + l = 4n + 2$ reflections would reduce the symmetry to the same $R3$ symmetry found at low temperatures [12]. The development of domains of lower symmetry than cubic also explains the reflection broadening (Fig. 2) as being the result of unresolved splitting.

Pressure evolution of Raman scattering reveals a sequence of reversible changes in the *local structure*, on a time scale much shorter than that of the dynamic fluctuations of polar nanoclusters. The Raman peaks observed at

FIG. 2. Pressure dependence of the pseudocubic unit-cell volume normalized to the volume at ambient pressure, f-F plot, and elastic bulk modulus K versus pressure.
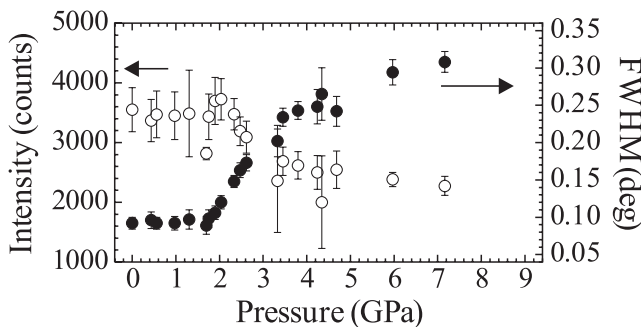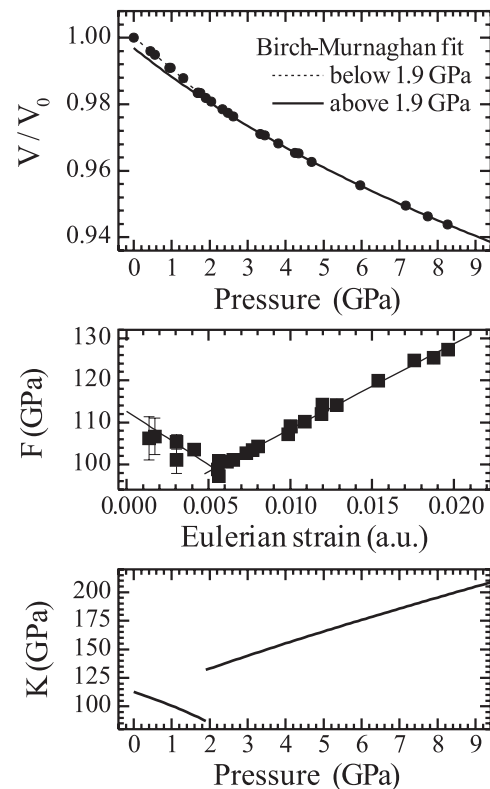
FIG. 1. Pressure dependence of the intensity and FWHM of the (022) Bragg reflection (indexed in $Fm\bar{3}m$). Other reflections show similar broadening. There is no systematic variation in FWHM with either reflection class or 2θ.
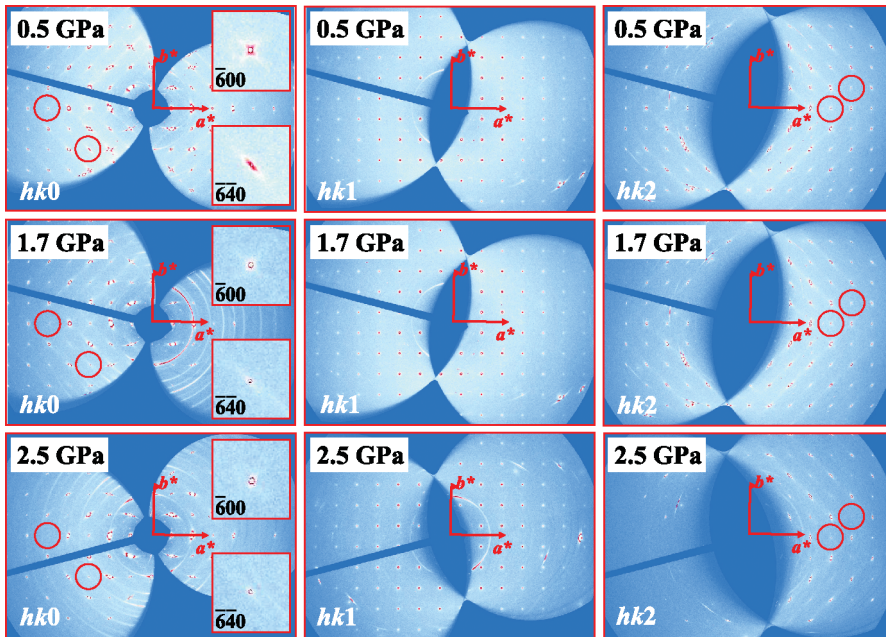
FIG. 3 (color). Reciprocal lattice reconstructions of synchrotron XRD data; additional datasets at 1.5, 1.9, 2.1, and 2.8 GPa show analogous features. The red circles mark example diffraction maxima of type $h + k + l = 4n + 2$, which exhibit a significant decrease in intensity as pressure is increased to 1.9 GPa, and are absent at higher pressures.

ambient pressure were unambiguously assigned to specific atomic vibrations on the basis of comprehensive polarized Raman studies of stoichiometric and doped PST and $PbSc_{0.5}Nb_{0.5}O_3$ [12]. At 1.2 GPa the peak near 135 cm^{-1} splits in two (Fig. 4). This peak is generated by rhombohedrally distorted BO_3-Pb species (see Fig. 4, the inset on right) and arises from a single rhombohedral mode related to the F_{1u} translational mode of the prototype structure $Fm\bar{3}m$, which involves motions of the BO_3 units against Pb atoms [12]. Hence, the splitting of this peak indicates a violation of the dynamical coupling between the Pb- and the B-cation system in the polar nanoregions. Near 1.2 GPa the pressure dependence of the wave number $\omega(p)$ for the scattering near 355 cm^{-1} has a kink (Fig. 5). This Raman signal is due to noncoplanarity of Pb and O atoms within {111} planes and it is sensitive to Pb-O bond stretching interactions within the Pb-O layers [12]. Hence, the change in the $\omega(p)$ slope indicates that the rate of stiffening of the Pb-O bonds within the {111} planes with pressure is increased above 1.2 GPa. On further pressure increase up to 1.9 GPa the higher-wave number component of the BO_3-Pb translational mode rapidly shifts to higher wave numbers (Figs. 4 and 5). Above $p_c = 1.9$ GPa a new Raman peak near 37 cm^{-1} is clearly observed (the left inset in Fig. 4), which arises from a soft mode associated with the phase transition detected by XRD. Apparently, the soft mode comprises vibrations of the heavy Pb atoms and its occurrence confirms the conclusion based on XRD data that the high-pressure phase is characterized by ordered Pb displacements. Near p_c the peak at 240 cm^{-1} drops in intensity (Fig. 5). This peak is related to the F_{1u} mode of $Fm\bar{3}m$ localized in B-site cations and its anomalous Raman activity is due to the existence of B-cation off-centered shifts [12]. These spectral changes show that the loss of coupling between Pb and B-cation systems allows

the displaced B cations to move back to the octahedral centers and the structure relaxes via enhancement of the structural anisotropy in the Pb system as would be expected for a symmetry change to $R3$. However, Raman
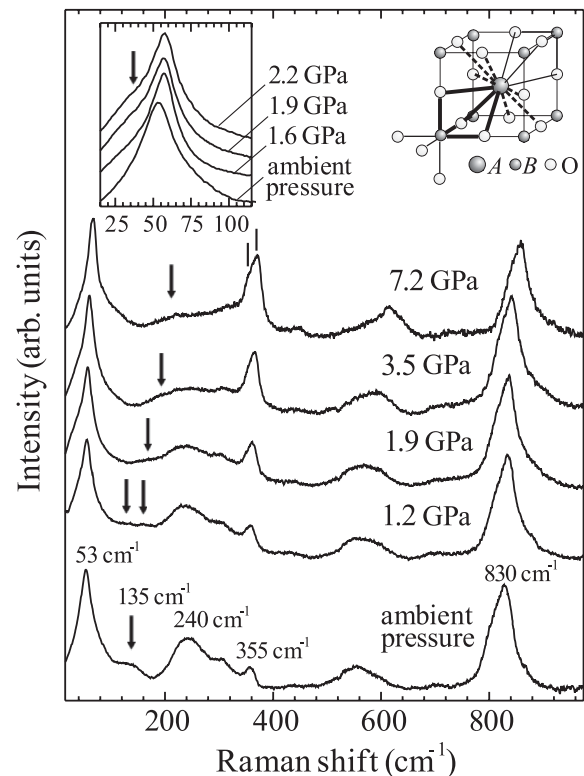

FIG. 4. Raman spectra of PST at different pressures; the arrows near 135 cm^{-1} in the main plot mark the Raman scattering arising from the BO_3-Pb translational mode; the lines near 355 cm^{-1} indicate the splitting of this peak. The arrow in the inset on the left indicates the soft mode near 37 cm^{-1}. The inset on the right represents structural species in the ABO_3 structure.
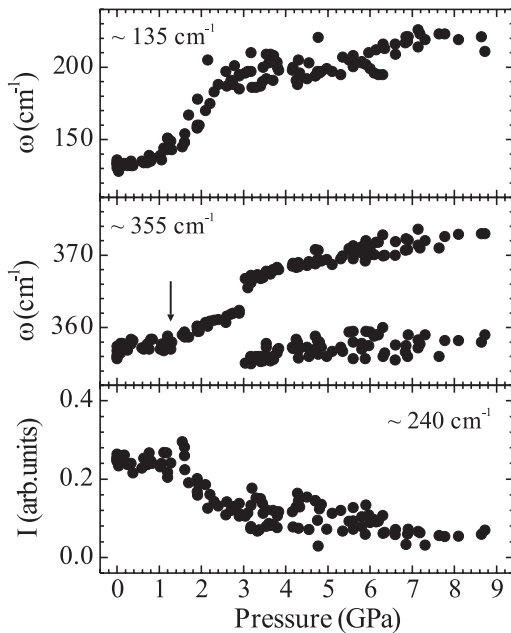
FIG. 5. Pressure dependence Raman peak positions (ω) and intensities (I) determined by fitting the spectra with Lorentzians. The plots represent data collected from different samples. The absolute error in ω and I is within the statistical deviation.

scattering reveals that the high-pressure local structure differs from that at low temperature. The observed decoupling between Pb and B-cation displacements and further suppression of B-cation off-center shifts indicates pressure-induced fragmentation of polar nanoregions existing at ambient pressure and is in accordance with the changes in dielectric permittivity at moderate pressures [2]. The decrease in intensity of the B-localized mode continues up to 3 GPa (Fig. 5). At that pressure a splitting of the Pb-O mode near 355 cm^{-1} occurs (Figs. 4 and 5), which points to a further enhancement of the ferroic distortion in the Pb-O system. Slightly above 3 GPa a small change in the $\omega(p)$ slope of the peak near 830 cm^{-1}, arising from BO_6 symmetrical stretching appears (not shown), revealing a decrease in the average BO_6 octahedral compressibility. Note that the pressure range of local structural changes above p_c corresponds to the pressure range of gradual weakening of the diffuse scattering. No further pressure-induced structural alterations were deduced from the Raman spectra up to 9 GPa.

In conclusion, initial compression of PST near T_m occurs by bond shortening. Eventually, volume reduction can no longer be accommodated by the bond shortening and the framework undergoes a continuous phase transition at 1.9 GPa associated with an elastic instability that is typical of octahedral tilt transitions in perovskites. The XRD data are consistent with the HP phase having the same *average* symmetry, $R3$, as that found at low temperature [13]. This would result in a positive slope of the equilibrium phase boundary in p-T space, in accordance with the principles governing tilt transitions in perovskites [14] were PST to

behave as a normal "2:4" perovskite. The tilted octahedra then allow ferroic ordering of the Pb atoms on a macroscopic length scale. The development of complete long-range order of the Pb displacements is continuous as evidenced by the persistence of the diffuse scattering immediately above the transition. The pressure-induced atomic rearrangements in PST, namely, Pb shifts that correlate within {111} planes and chains of antiphase tilted octahedra with suppressed B-cation *polar* off-shifts, should be characteristic of all Pb-based relaxors and explain the disappearance of x-ray diffuse scattering above a certain pressure [4]. This interpretation is in a full agreement with the Raman spectra showing that the displacements of the B-site cations in the existing dynamical polar nanoclusters are suppressed in the HP phase whereas the local noncubic displacement of ferroic Pb-O species is enhanced. For PST the structural changes are clearly observed by both diffraction and Raman scattering because of the longer coherence length of ferroic Pb-O species that is already apparent at ambient conditions [12].

*Corresponding author.
mi0a007@uni-hamburg.de
†Corresponding author.
rangel@vt.edu

[1] A. A. Bokov and Z.-G. Ye, J. Mater. Sci. **41**, 31 (2006).
[2] G. A. Samara, Phys. Rev. Lett. **77**, 314 (1996); E. L. Venturini *et al.*, Phys. Rev. B **74**, 064108 (2006); G. A. Samara and E. L. Venturini, Phase Transit. **79**, 21 (2006).
[3] G. Xu *et al.*, Phys. Rev. B **69**, 064112 (2004); M. Pasciak, M. Wolcyrz, and A. Pietraszko, *ibid.* **76**, 014117 (2007).
[4] B. Chaabane *et al.*, Phys. Rev. Lett. **90**, 257601 (2003); M. Ahart *et al.*, Phys. Rev. B **71**, 144102 (2005); P.-E. Janolin *et al.*, *ibid.* **73**, 094128 (2006).
[5] J. Kreisel *et al.*, Phys. Rev. B **65**, 172101 (2002); B. Chaabane *et al.*, *ibid.* **70**, 134114 (2004); A. Sani *et al.*, *ibid.* **69**, 020105(R) (2004).
[6] Y. Yan *et al.*, Appl. Phys. Lett. **72**, 3145 (1998).
[7] R. J. Angel *et al.*, J. Appl. Crystallogr. **30**, 461 (1997).
[8] R. J. Angel *et al.*, J. Appl. Crystallogr. **40**, 26 (2007).
[9] R. G. Munro *et al.*, J. Appl. Phys. **57**, 165 (1985).
[10] M. A. Carpenter and E. K. H. Salje, Eur. J. Mineral. **10**, 693 (1998).
[11] C. J. Howard, B. J. Kennedy, and P. M. Woodward, Acta Crystallogr. Sect. B **59**, 463 (2003).
[12] B. Mihailova *et al.*, J. Phys. Condens. Matter **14**, 1091 (2002); B. Mihailova *et al.*, *ibid.* **19**, 246220 (2007); B. Mihailova *et al.*, *ibid.* **19**, 275205 (2007).
[13] P. M. Woodward and K. Z. Baba-Kishi, J. Appl. Crystallogr. **35**, 233 (2002).
[14] R. J. Angel, J. Zhao, and N. L. Ross, Phys. Rev. Lett. **95**, 025503 (2005).